Fuel 268 (2020) 117342

Contents lists available at ScienceDirect

Fuel

journal homepage: www.elsevier.com/locate/fuel

Full Length Article

Comparison of pyrolysis of live wildland fuels heated by radiation vs. convection☆

Mohammad-Saeed Safdari[a], Elham Amini[a], David R. Weise[b], Thomas H. Fletcher[a,*]

[a] Chemical Engineering Department, 330 EB, Brigham Young University, Provo, UT 84602, USA
[b] USDA Forest Service, PSW Research Station, Fire and Fuels Program, Riverside, CA, USA

GRAPHICAL ABSTRACT

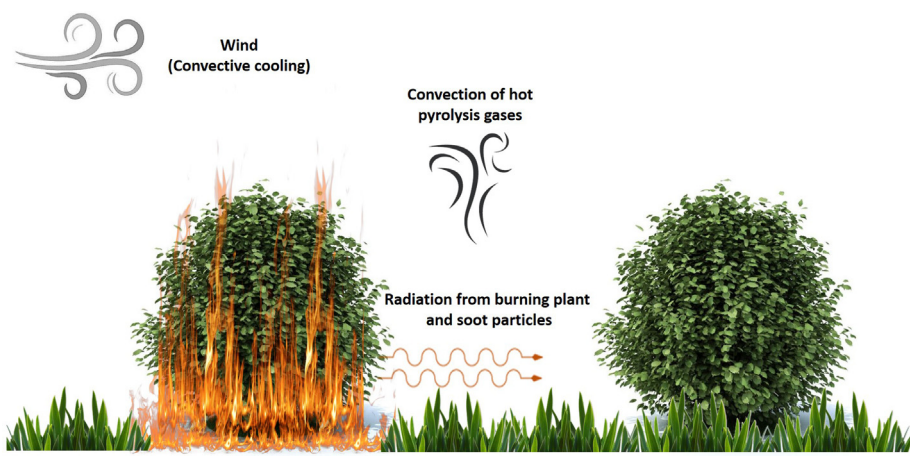

ARTICLE INFO

Keywords:
Pyrolysis
Heat transfer mechanism
Radiation
Convection
Tar
Light gas

ABSTRACT

During wildland fires, which include both planned (prescribed fire) and unplanned (wildfire) fires, live and dead plants may be subject to both radiative and convective heat transfer mechanisms. In this study, the pyrolysis of 14 live plant species native to the forests of the southern United States was investigated using a flat-flame burner (FFB) apparatus under three heating modes in order to mimic pyrolysis of plants during wildland fires. The heating modes were: (1) radiation-only, where the plants were pyrolyzed under a moderate heating rate of 4 °C s^{-1} (radiative flux of 50 kW m^{-2}); (2) convection-only, where the FFB apparatus was operated at a high heating rate of 180 °C s^{-1} (convective heat flux of 100 kW m^{-2}); and (3) a combination of convection and radiation, where the plants were exposed to both convective and radiative heat transfer mechanisms. Data were also compared with slow heating experiments (0.5 °C s^{-1}). During the experiments, the pyrolysis products were collected and analyzed using GC–MS for the analysis of tars and GC-TCD for the analysis of light gases. The results indicate that the highest light gas and tar yields were obtained from the combined mode, which was performed at a higher pyrolysis temperature and heating rate. CO, CO_2, CH_4, and H_2 were the major light gas species in all three heating modes. The radiation-only mode led to formation of primary tars and a few secondary tars consisting of aliphatic and 1–2 ring aromatic compounds with 1 to 3 attachments, including alkyl, hydroxyl, and methoxy groups.

☆ This manuscript was prepared, in part, by a U.S. Government employee on official time, is not subject to copyright and is in the public domain.

* Corresponding author.
E-mail address: tom_fletcher@byu.edu (T.H. Fletcher).

https://doi.org/10.1016/j.fuel.2020.117342
Received 2 October 2019; Received in revised form 4 February 2020; Accepted 5 February 2020
Available online 12 February 2020
0016-2361/ © 2020 Elsevier Ltd. All rights reserved.

1. Introduction

During wildland fires, which include both planned (prescribed fire) and unplanned (wildfire) fires, plants lose moisture content due to evaporation and undergo a two-step thermal degradation process (pyrolysis and combustion) when exposed to high temperatures [1,2]. In order to improve prescribed fire application, accomplish desired fire effects, and limit potential runaway fires, an improved understanding of the fundamental processes related to pyrolysis and ignition of plants is needed. The pyrolysis of plants is a thermal decomposition process, which does not require the presence of oxygen. As pyrolysis gases leave the surface of the plant, the mass transfer pushes the surrounding gas (presumably air) out of the way, providing a fuel-rich (pyrolysis) zone near the surface of the plant or in the interior of a flame. Pyrolysis products may later react with O_2 at high temperatures, and form flames in the presence of an ignition source [3–5].

During wildland fires, plants are pyrolyzed and burned through very complex heat transfer mechanisms [6]. As shown in Fig. 1, heat transfer mechanisms in wildland fires are: (1) convective heat transfer from hot gases to plants, especially for wind-driven fires; (2) radiative heat transfer from burning plants; and (3) radiative heat transfer from flames [7]. Radiative and convective heat transfer mechanisms are the two most dominant types of heat transfer mechanisms in wildland fires [8].

The convective heat transfer mechanism is essential for pyrolysis, ignition of plants, and wildland fire spread [9]. Convection from hot post-combustion gases heat plants that then give off moisture and pyrolysis products. The pyrolysis products can later react with oxygen in the presence of an ignition source and burn. The heat from combustion of the pyrolysis products is transferred to surrounding plants, starting the evaporation and pyrolysis processes for those plants. This process repeats continuously and propagates the fire [10]. Radiant heat energy is transferred from: (1) hot soot particles in the flame; (2) burning solid fuels such as charred leaves, tree bark, and branches; and (3) hot gases consisting mainly of post-combustion gases such as H_2O and CO_2. Soot in wildland fires is mainly formed by the polymerization of polycyclic aromatic compounds in the pyrolyzed tar. Radiative heat flux decreases exponentially relative to the distance from the flames [11].

In order to develop predictive models, it is important to understand how convection and radiation contribute to the pyrolysis and combustion of live and dead plants. The relative contribution of convective and radiative heat transfer mechanisms are complicated and not well understood [11]. There is still a lack of consensus among researchers regarding the dominant heat transfer mechanism in wildland fires [12]. Some previous researchers proposed that a combination of convective and radiative heat transfer mechanisms plays a role in fire spread [6,13], whereas others have demonstrated that radiation is only important in plant preheating [10,14]. More recent small-scale studies have indicated that radiative heat transfer, at the levels experienced in wildland fires, is not sufficient to ignite the plants [15]. However, ignition of plant species can occur via convective heat transfer through hot gases without an ignition source [16]. Furthermore, it has been proposed that convection or direct flame-fuel contact is important in fire spread, especially in windy conditions [15,17–25]. Rothermel [26] showed that radiation from both burning particles and hot gases is more important in pre-heating plants during no-wind conditions and backing fires (when fire spreads against wind). In contrast, convection dominates in pre-heating plants in heading fires (when fire spreads with wind) [1,11]. The lack of consensus among researchers regarding the dominant heat transfer mechanism is likely caused by the different data sets that have been collected in various experimental conditions.

Many studies have been performed during the past few decades regarding the combustion of wildland fuels. However, there is still a major gap in the understanding of the effects of different heating modes on the production and composition of pyrolysis products. In this study, the effects of convective and radiative heat transfer mechanisms on the yields and the compositions of pyrolysis products from 14 live plant species were investigated. Fourteen plant species native to the pine forests of the southern United States where prescribed burning is used were selected.

The experiments were performed in a flat-flame burner (FFB) apparatus to mimic pyrolysis of plants during wildland fires. The FFB apparatus was operated under three heating modes to investigate the effects of different heat transfer mechanisms on the yields and the

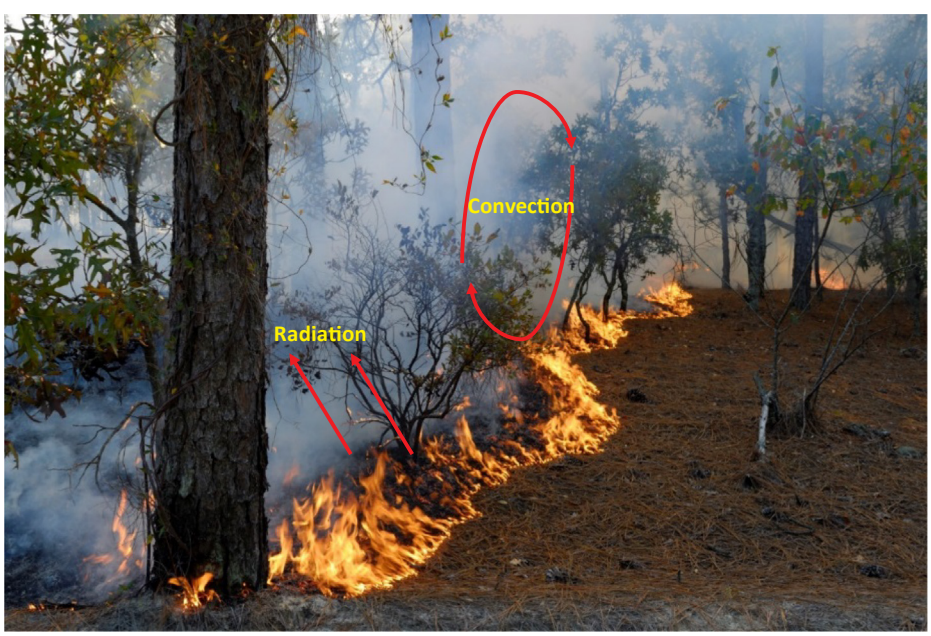

Fig. 1. Heat transfer mechanisms in wildland fires. Taken from [4].

compositions of pyrolysis products. The heating modes were: (1) radiation-only; (2) convection-only; and (3) a combination of radiation and convection. During the experiments, pyrolysis products were collected and analyzed using GC–MS for the analysis of tars and GC-TCD for the analysis of light gases. The results of the convection-only experiments were previously published [5] and then compared with results on the same species at low heating rates [27]. The purpose of this paper is to compare the data from radiation-only and combined radiation and convection experiments with the previous convection-only and slow heating data in order to explore effects of temperature, heating rate, and pyrolysis environment.

2. Material and methods

2.1. Fuels tested

Table 1 lists the plants used in the pyrolysis experiments. The plants were nursery-grown in Florida and then were express-mailed to the combustion laboratory at Brigham Young University (BYU). Images, proximate and ultimate analyses, and physical properties of these species can be found elsewhere [4,5]. Unlike typical pyrolysis experiments, in these experiments, all samples were left intact with no grinding or crushing in order to prevent early escape of volatile components in the plant structure.

2.2. Experimental setup and procedure

A flat-flame burner (FFB) apparatus (as shown in Figs. 2 and 3) was used to study the pyrolysis of these plants under three different heating modes. The heating modes were: (1) radiation-only, where the plants were pyrolyzed at a moderate heating rate of 4 °C s^{-1} (radiative flux of 50 kW m^{-2}) and a maximum fuel surface temperature of 550 °C. Nitrogen flowed from the burner as a carrier gas, but the burner was not ignited; (2) convection-only, where the FFB apparatus was operated at a high heating rate of 180 °C s^{-1} (convective heat flux of 100 kW m^{-2}) and a maximum fuel surface temperature of 750 °C to imitate pyrolysis under convective heat transfer; and (3) a combination of radiation and convection, where the plants were exposed to both convective and radiative heat fluxes. In the combined mode, the maximum heating rate was calculated to be approximately 195 °C s^{-1}. The maximum fuel surface temperature was 750 °C for the convection-only mode, 550 °C for the radiation-only mode, and 800 °C for the combined mode. The heat fluxes which were used in the pyrolysis experiments were the maximum values that could be obtained from the flat-flame burner apparatus and the radiation panel. Data from a slow heating experiment (0.5 °C s^{-1} in N_2 to different temperatures) were published previously [3] and are also used for comparison. The slow heating rate experiments were performed using the pyrolyzer apparatus, which was equipped with a metal tube and an electrically-heated programmable furnace. The tar and gas collection system in the pyrolyzer system was identical to that used in the FFB system. The details of the apparatus and its operating conditions were presented elsewhere [3]. Admittedly, it would have been nice to perform all of the experiments at the same surface temperature and net heat flux, but this was not possible.

For modes (2) and (3) where the effects of convective heat were studied, in order to provide pyrolysis conditions and an oxygen-free environment (i.e., no sample combustion), the FFB was operated in a fuel-rich mode (equivalence ratio: $\Phi = 1.13$). A mixture of CH_4 and H_2 comprised the burner fuel, which was oxidized with atmospheric air. The samples were heated convectively by the post-flame burner products (CO_2, H_2O, and CO).

For modes (1) and (3), where the effects of radiative heat were investigated, an OMEGALUX QH-101060[1] infrared radiant heating panel was used (as shown in Fig. 3). The radiant heating panel used a fused quartz glass emitter face. The panel was connected to a temperature controller. By adjusting the set point to 600 °C, the panel emitted radiation at an output wavelength between 2.5 and 6 μm and a constant heat flux of 50 kW m^{-2}. For mode (1), where the effects of only radiative heat transfer were studied, 16.6 L min^{-1} N_2 flowed as a carrier gas through the burner to provide an oxygen-free environment in the system while the burner was not ignited. Table 2 summarizes the operating conditions during the experiments.

The radiative and convective heat fluxes were measured by a calibrated Medtherm 64-series total heat flux sensor (radiometer). The average gas temperature within the FFB at the height where the sample was located was measured using a K-type thermocouple. In addition, the plant surface temperature was recorded by an FLIR A-300 Series infrared camera, and the data analysis was performed using FLIR Research IR Max 4 software. The average heating rates were calculated by finding the difference between the maximum fuel temperature (from IR temperature data) and room temperature (25 °C) divided by the corresponding time elapsed to reach the maximum temperature. The detailed description of how the samples were loaded in the FFB apparatus and how the pyrolysis products were collected and analyzed can be found elsewhere [3–5].

Table 1
List of plants used in pyrolysis experiments.

Scientific name	Common name	Growth form
Aristida stricta Michx.	Wiregrass	Grass
Ilex glabra (L.) A. Gray	Inkberry	Shrub
Ilex vomitoria Aiton 'Schelling Dwarf'	Yaupon	Shrub
Lyonia lucida (Lam.) K. Koch	Fetterbush	Shrub
Morella cerifera (L.) Small	Wax myrtle	Shrub
Persea palustris (Raf.) Sarg.	Swamp bay	Shrub
Pinus palustris Mill.	Longleaf pine foliage	Tree
Pinus palustris Mill.	Longleaf pine litter	Tree
Quercus nigra L.	Water oak	Tree
Quercus virginiana Mill.	Live oak	Tree
Sabal minor (Jacq.) Pers.	Dwarf palmetto	Shrub
Schizachyrium scoparium (Michx.) Nash	Little bluestem	Grass
Serenoa repens (W. Bartram) Small	Saw palmetto	Shrub
Vaccinium arboreum Marshall	Sparkleberry	Shrub
Vaccinium darrowii Camp "Rosa's Blush"	Darrow's blueberry	Shrub

3. Results and discussion

3.1. Fuel surface temperature

Infrared images taken using an IR camera during the pyrolysis of the leaves indicate that the leaves did not heat isothermally under three different heating modes (as illustrated in Fig. 4). Different angles of the leaves in the pictures were due to the location of the IR camera. For the radiation only experiments, the IR camera was placed above the FFB looking down (Fig. 4a), but for the convection-only and the combined mode the IR camera was placed on one side of the FFB. At the beginning of the experiments, there were temperature gradients within the leaves; the edges of the leaves had higher temperatures than the middle of the leaves. As time passed, the heat traveled from the edges towards the center until the temperature was uniform across the entire leaf. Live plants started to pyrolyze from the edges and proceed towards the center. The maximum fuel surface temperatures for the radiation-only, convection-only, and the combined modes, were 550, 750, and 800 °C, respectively, as measured by the IR camera. For the radiation-only mode, a uniform temperature across the entire leaf was observed after

[1] The use of trade or firm names in this publication is for reader information and does not imply endorsement by the U.S. Department of Agriculture of any product or service.

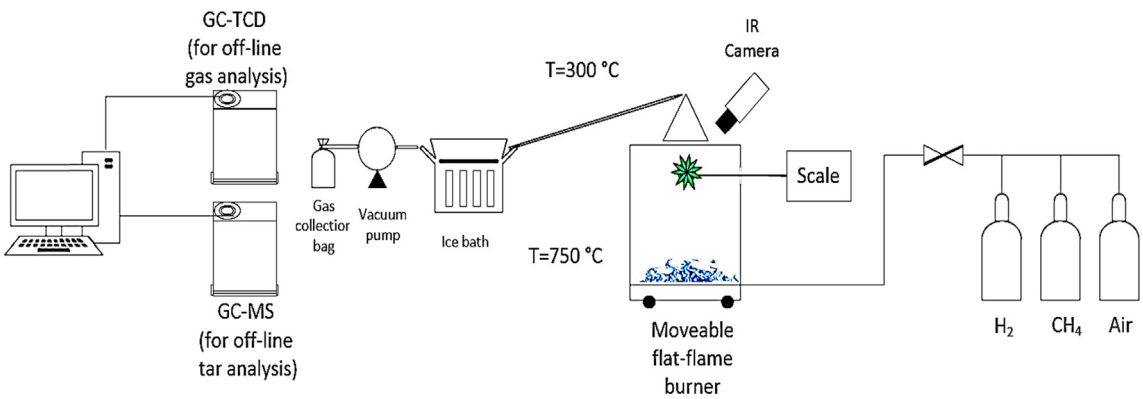

Fig. 2. Flat-flame burner apparatus. Taken from [5].

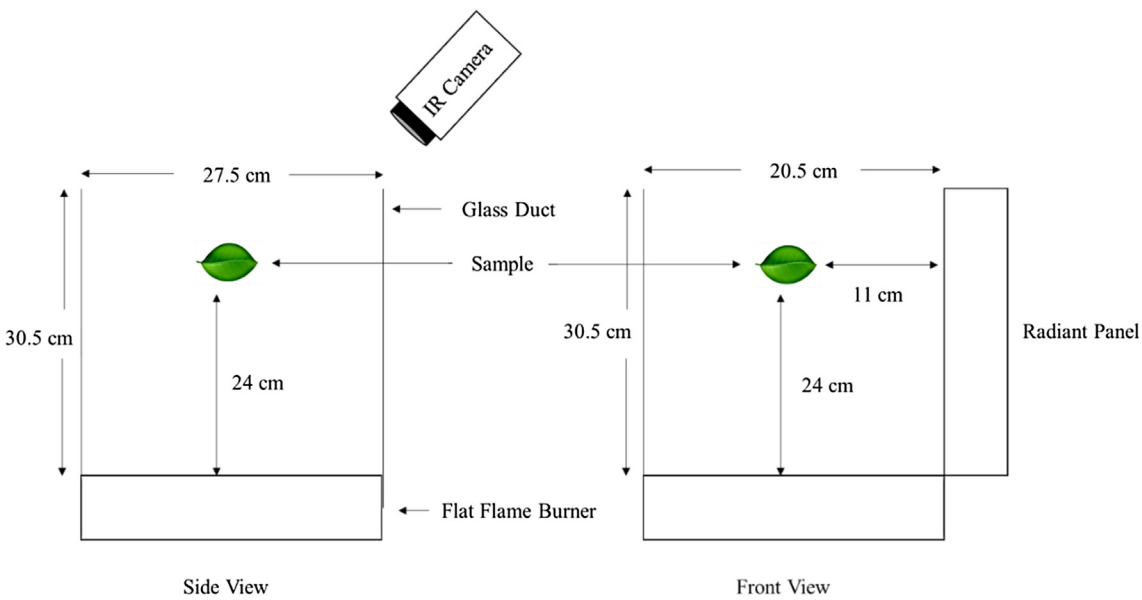

Fig. 3. Schematic of the FFB [4]

Table 2
Operating temperature and heat flux in the experiments.

Heating modes	Apparatus	Radiative heat flux	Convective heat flux	Average heating rate	Average gas temperature	Fuel surface temperature
Slow heating	Pyrolyzer	n.a.	n.a.	0.5 °C s^{-1}	Varies	varies
Radiation-only	FFB	50 kW m^{-2}	0 kW m^{-2}	4 °C s^{-1}	105 °C	550 °C
Convection-only	FFB	0 kW m^{-2}	100 kW m^{-2}	180 °C s^{-1}	765 °C	750 °C
Conv. and Rad.	FFB	50 kW m^{-2}	100 kW m^{-2}	195 °C s^{-1}	804 °C	800 °C

120 s. However, this equilibration time was approximately 4 s for the convection-only and the combined modes, due to the higher heat flux. The convection-only image (Fig. 4b) still has some temperature gradients in the center of the leaf at 4 s, while the leaf in the combined mode at 4 s is fairly uniform, indicating that the combined mode results in a slightly faster heating rate and shorter time to uniform temperature than in the convection-only mode.

3.2. Pyrolysis product yields

The pyrolysis product yield data (i.e., light gas yield, tar yield, and char yield) from the pyrolysis of the live plant species using the four heating modes are presented in this section. All the results compared in this study are the average of three repetitions and the error bars in the figures represent the ± 95% confidence intervals for three repetitions. Previous studies have shown that temperature and heating rate have significant impacts on the yields of pyrolysis products [27–33].

A complete set of product yield data for all 14 species is given in the supplementary material. A summary of the product yields from the four heating modes is given in Table 3 for the live plant species, where the ranges represent the lowest and highest values in the data set. The final pyrolysis temperatures in the slow-heating and radiation-only modes were very similar (500 vs 550 °C), which seems to explain why the light gas yields were similar. However, tar yields were generally higher in the radiation only experiments, and char yields were higher in the pyrolyzer. The higher temperatures and heating rates in the convection-only and combined modes generally resulted in higher tar and light gas yields, and hence lower char yields. Light gas yields were highest and char yields were lowest in the combined mode. Higher gas and tar yields at the higher heating rates and temperatures were due to the further pyrolysis of char and secondary pyrolysis reactions at higher temperatures and heating rates [31,34–37].

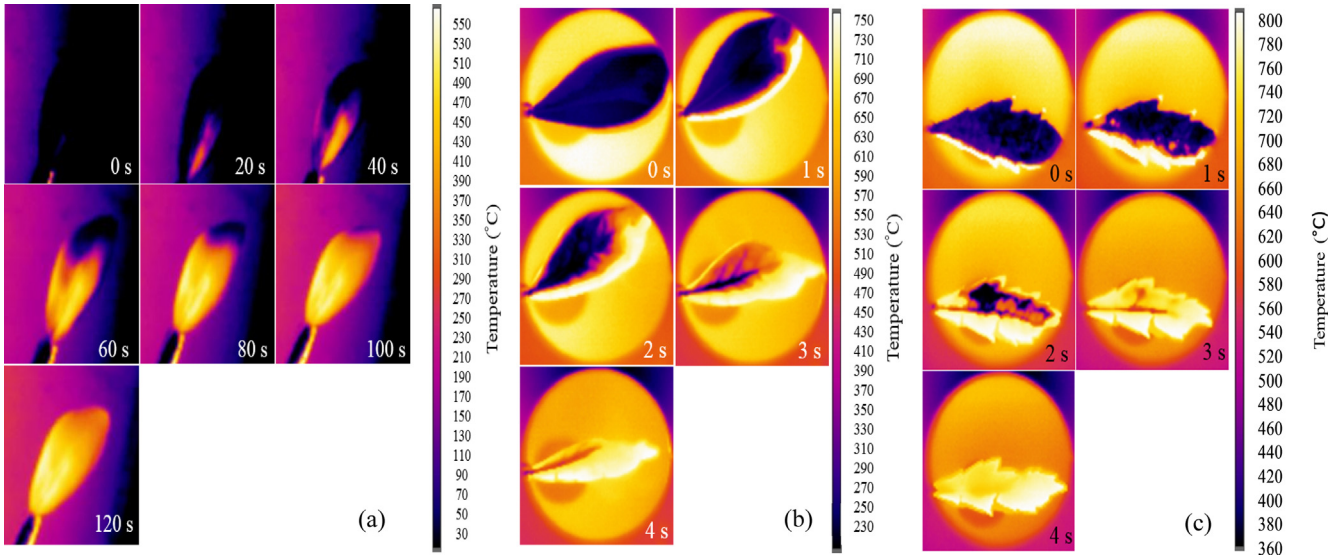

Fig. 4. Fuel surface temperature over time for (a) the radiation-only mode (inkberry), (b) the convection-only mode (inkberry, different view angle), and (c) the combined mode (wax myrtle).

Table 3
Summary of pyrolysis product yields for live species for four heating modes.

Heating modes	Apparatus	Tar yield[a]	Light gas yield[a]	Char yield[a]
Slow Heating to 500 °C [27]	Pyrolyzer	44–54	16–24	27–34
Radiation-only	FFB	49–57	16–23	24–29
Convection-only [27]	FFB	53–62	18–25	17–22
Convection and Radiation	FFB	55–63	20–27	14–19

[a] wt% on a dry, ash-free (daf) basis.

The differences in product yields as summarized in Table 3 may be due to temperature, heating rate, or residence time. Heating rate and residence time are closely related. One set of slow heating experiments was performed at a broader range of temperatures in order to compare the temperature effect on pyrolysis product yields. Pyrolysis data for longleaf pine litter were obtained in a pyrolyzer at 0.5 °C/s at temperatures up to 800 °C by Amini et al. [3]. Ignoring heating rate, the pyrolysis product yields for longleaf pine litter are plotted vs. final temperature in Fig. 5.

The higher heating rate experiments were expected to have higher total volatiles yields than the slow heating rate experiments. However, in these experiments, the low heating rate experiments at 500–600 °C showed higher conversion to volatiles than observed in the radiation-only experiments in the FFB system. At higher temperatures (750–800 °C), the total volatile yield from the low and high heating rate experiments were the same, within experimental error. It was also expected that the tar yield temperatures above 500 °C would decrease, due to secondary tar reactions [38]. The decrease in tar yield was observed in the low heating experiment (solid line with triangles), with a corresponding increase in light gas yield. This decrease in tar yield with an increase in light gas yield can be explained largely by conversion of tar to light gas by cracking of heavy molecules to make light molecules. However, the tar yield in the FFB system increased with increasing temperature, as did the light gas yield. Certainly the heating rates were higher in the convection and convection plus radiation modes of heating than in the pyrolyzer, which may have had an effect. The residence time of tar in the system at hot temperatures was also much different between the FFB system and the pyrolyzer system. In any case, the difference in product yields cannot be explained merely by temperature.

3.2.1. Light gas yields

Light gas yields for each species in each heating mode are given in Fig. A-1 (i.e., Fig. 1 in the appendix). The average gas yield obtained from the pyrolysis of all plants was 20 wt% (daf) for the slow-heating and radiation-only modes, 22 wt% for the convection-only mode, and 24 wt% for the combined mode. For most of the plants, the confidence intervals of the light gas yield data from the convection-only mode overlap the data from the combined mode, showing that the difference between these two heating modes was not statistically significant.

The highest gas yields for each heating mode were observed during the pyrolysis of: (1) saw palmetto in the radiation-only mode (23 wt%); (2) saw palmetto in the convection-only mode (25 wt%); and (3) fetterbush (27 wt%) followed by saw palmetto (26 wt%) in the combined mode. Wax myrtle showed the largest difference between the gas yields for the radiation-only and the combined modes (5 wt%). The high light gas yield seen in the convection-only and the combined modes is partially due to the higher sample temperature, and may be partially due to the further cracking of char and secondary reactions of tar that occurs at higher pyrolysis temperatures and heating rates [39,40]. In addition, since the post-flame gases in the FFB contain CO_2 and H_2O, there is a possibility that some heterogeneous gasification of the char sample may

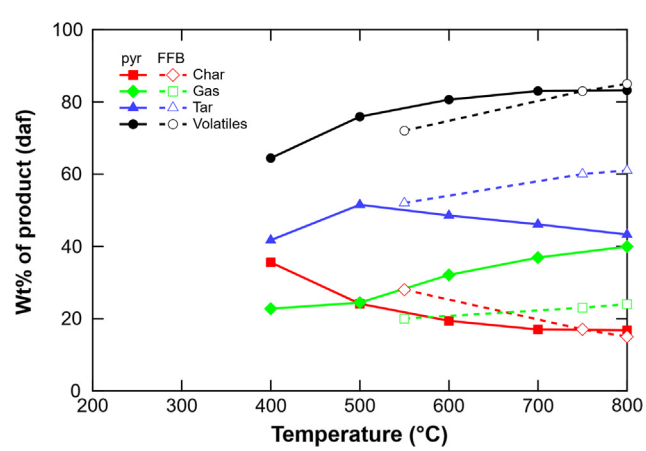

Fig. 5. Comparison of pyrolysis product yields vs. final temperature for data from a pyrolyzer (solid lines) at 0.5 °C/s [3] and from the flat flame burner system (dashed lines) under different modes of heating (radiation only, convection only, and radiation plus convection, see Table 2).

have occurred, resulting in higher light gas yields. However, this gasification effect is thought to be small due to the small residence times and relatively moderate temperatures (compared to commercial gasifiers) in the FFB experiments.

3.2.2. Tar yields

The tar yields for the three heating modes are shown in Figure A-2. Higher tar yields were obtained by increasing the pyrolysis temperature and heating rate. The tar yield data from the convection-only mode were closer to the results of the combined mode than to the results of the radiation-only mode, similar to the results seen in the light gas yield data. The tar yield data from the slow-heating and radiation-only modes showed non-overlapping confidence intervals with the two other heating modes, indicating that the difference between the tar yields from the slower heating experiments and the faster heating experiments was statistically significant. The average tar yield from the pyrolysis of all plants was 49 wt% (daf) for the slow-heating mode and 53 wt% (daf) for the radiation-only mode. However, this value was 58 and 59 wt% (daf) for the convection-only and the combined modes, respectively. Among all of the plant species, dwarf palmetto showed the highest tar yield for all four heating modes: (1) 54 wt% in the slow-heating mode; (2) 57 wt% in the radiation-only mode; (3) 62 wt% in the convection-only mode; and (4) 63 wt% in the combined mode. The largest difference between tar yield data sets was observed during the pyrolysis of longleaf pine foliage with a difference of 9 wt% in tar yields from the radiation-only and the combined modes.

The tar yield data indicate that the plants from the same family (i.e., (i) live oak and water oak, (ii) inkberry and yaupon, and (iii) sparkleberry and Darrow's blueberry) produced very similar tar yields in the experiments. For example, tar yields for water oak and live oak were 47 and 45 wt% in the slow-heating mode, 53 and 54 wt% in the radiation-only mode, 56 and 57 wt% in the convection-only mode, and 58 and 60 wt% in the combined mode. Josephson et al. [41] showed that the fraction of volatiles in fuel and the size of tar can be predicted by surrogate models.

3.2.3. Char yields

As shown in Figure A-3, the char yields decreased as the pyrolysis temperature and the heating rate increased, which is consistent with the gas and tar yield data. Similar observations have been reported in previous studies [42–45]. For all of the plant species, the char yield data from the radiation-only mode showed non-overlapping confidence intervals with the results from the two other heating modes, indicating a significant difference between the char yields obtained in these heating modes. The char yields from the slow-heating mode showed non-overlapping confidence intervals with the radiation-only mode for most species. The highest char yields for each heating mode were observed during the pyrolysis of: (1) sparkleberry and live oak (34 wt%) in the slow-heating mode; (2) sparkleberry (29 wt%) in the radiation-only mode; (2) sparkleberry (23 wt%) in the convection-only mode; and (3) saw palmetto (19 wt%) in the combined mode. The largest difference between the char yield data was observed in the pyrolysis of longleaf pine foliage between the radiation-only and the combined modes (13 wt%).

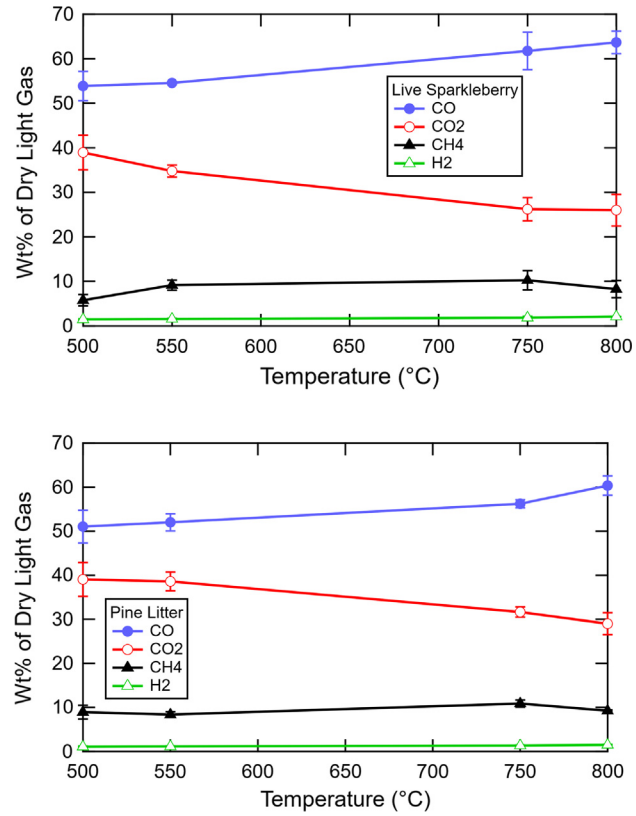

Fig. 6. Light gas species observed during pyrolysis of live sparkleberry (top) and pine litter (bottom) plotted as a function of final temperature.

3.3. Light gas species analysis

The differences in light gas and tar yields shown above raise the question of which light gas species are changing with the different heating modes. The measured yields of light gas species for live plants in each of the four heating modes are given in Figures A-4-A-7. All values are reported as wt% of the dry light gas collected (i.e., excluding the tar and char). A summary of the light gas species yields is presented in Table 4. In most cases, weight fraction of CO increased by increasing the pyrolysis temperature and heating rate. The highest yields of CO were observed during the pyrolysis experiments performed under the combined mode. In contrast, weight fractions of CO_2 decreased with increased pyrolysis temperature and heating rate. The highest yields of CO_2were observed in the slower heating modes. Changes in the H_2 yields were small for the different modes of heating, and likely within experimental error. Note that the mole% of H_2 in the dry light gases was

Table 4
Summary of light gas analysis during pyrolysis of live plants for three heating modes.

Heating mode	Apparatus	H_2		CO		CO_2		CH_4	
		Avg[a]	Rng[b]	Avg	Rng	Avg	Rng	Avg	Rng
Slow-heating to 500 °C	Pyrolyzer	1.4	1.1–1.7	52.1	47–58	38.4	34–42	8.1	5–11
Radiation-only	FFB	1.5[c]	1.3–1.9	53.4	51–56	36.0	33–39	9.1	8–10
Convection-only	FFB	1.7	1.3–2.1	59.8	53–63	29.5	25–35	8.9	6–11
Convection and Radiation	FFB	2.0	1.7–2.4	63.6	60–66	26.8	25–30	7.6	6–8

[a] Average.
[b] Range.
[c] Wt% on a dry light gas-only basis.

much higher (15 to 20 mol%) than the wt% basis.

Representative light gas species data are shown in Fig. 6 for pyrolysis of live sparkleberry and dead pine litter. The results indicate that for all three heating modes, CO was the main light gas species on a wt% basis, followed by CO_2, CH_4, and H_2.

As shown in Fig. 6, the lowest CO yields were observed during the slow-heating modes (lowest temperatures) and the highest values were observed in the combined mode (highest temperature). This trend suggests that by increasing the temperature and heating rate, higher yields of CO can be obtained. The highest CO yields for each heating mode were observed during the pyrolysis of: (1) sparkleberry (50 wt%) in the slow-heating mode; Darrow's blueberry (56 wt%) in the radiation-only mode; (2) saw palmetto (63 wt%) in the convection-only mode; and (3) inkberry (66 wt%) in the combined mode. The little bluestem showed the largest difference in the CO yield (13 wt%) between different heating modes. At low pyrolysis temperatures, CO is formed mostly by the decomposition of hemicellulose and cellulose. However, at high pyrolysis temperatures, CO yield can be increased due to the cracking of carbonyl (C = O) and carboxyl (C(=O)OH) groups [46].

Carbon dioxide was the second most abundant light gas in all three heating modes. As shown in Fig. 6, CO_2 showed a different trend compared to CO when increasing the temperature and heating rate. The slow-heating modes (i.e., lowest temperatures) produced the highest CO_2 yields, while the convection-only and the combined modes resulted in lower yields of CO_2. The highest weight fractions of CO_2 for each heating mode were observed during the pyrolysis of: (1) little bluestem grass (42 wt%) in the slow-heating mode; (2) wax myrtle (43 wt%) in the radiation-only mode; (2) swamp bay (35 wt%) in the convection-only mode; and (3) dwarf palmetto (31 wt%) in the combined mode.

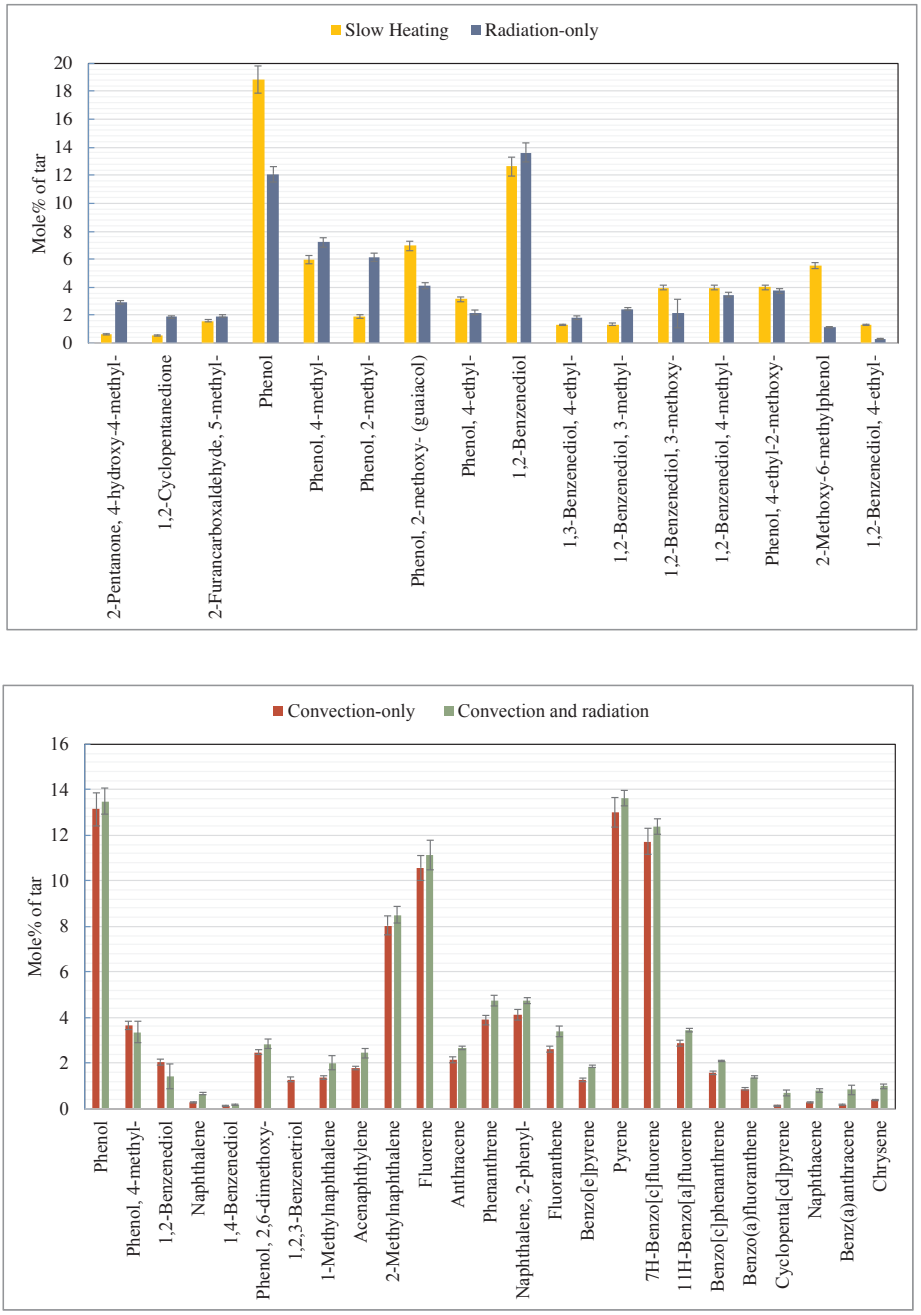

Fig. 7. Analysis of tar compounds from Longleaf pine needles in: the slow-heating (data from [27]) and radiation-only modes (top); the convection-only mode (data from [5]), and the combined modes (bottom).

Little bluestem showed the largest difference in the weight percent of CO_2 between different heating modes (12 wt%), followed by the water oak (11 wt%). CO_2 is mainly formed by the degradation of hemicellulose at low temperatures (< 500 °C) [47]. Only a small portion of CO_2 is thought to be formed due to the decomposition of cellulose. At higher temperatures (> 500 °C), CO_2 is mainly formed by the cracking and reforming of oxygen-containing functional groups in the lignin structure, such as carbonyl groups (C = O) and carboxyl groups (C(=O)OH) [28,46,48]. The average ratio of CO/CO_2 ratio (wt% basis) was 1.36 for the slow-heating and radiation-only modes, 1.92 for convection-only mode, and 2.38 for the combined mode. This indicates that by increasing the pyrolysis temperature and heating rate, the CO_2 yield constantly decreased with a corresponding increase in the CO yield.

Methane was the third most prevalent light gas species in all three heating modes. The complete results of the CH_4 yields are shown in Figure A-6. For most of the plants, higher yields of CH_4 were observed during the pyrolysis experiments performed under the radiation-only mode. However, for a few plant species, such as Darrow's blueberry and swamp bay, higher yields of CH_4 were obtained during the convection-only mode. The highest wt% of CH_4 belonged to the pyrolysis of little bluestem grass (12 wt%) under the convection-only mode. All the main structural components of plants can contribute to the formation of CH_4 during pyrolysis at all temperature ranges. However, lignin is thought to be the main contributor to CH_4 formation, which may be due to its high methoxy (O-CH_3) content [46].

As shown in Fig. 6, the average yields of H_2 varied from 1 to 2 wt% during all heating modes. For all plant species, the greatest H_2 yields were observed in the combined mode. Swamp bay showed the highest H_2 yield (2.4 wt%) in the combined mode. Among all plant species, swamp bay exhibited the highest H_2 weight percent difference (0.9 wt %) between the radiation-only and the combined modes. H_2 is mainly formed due to the dehydrogenation and radical polycondensation that occur throughout pyrolysis. At high pyrolysis temperatures, H_2 can be formed due to either the dehydrogenation reaction or the degradation

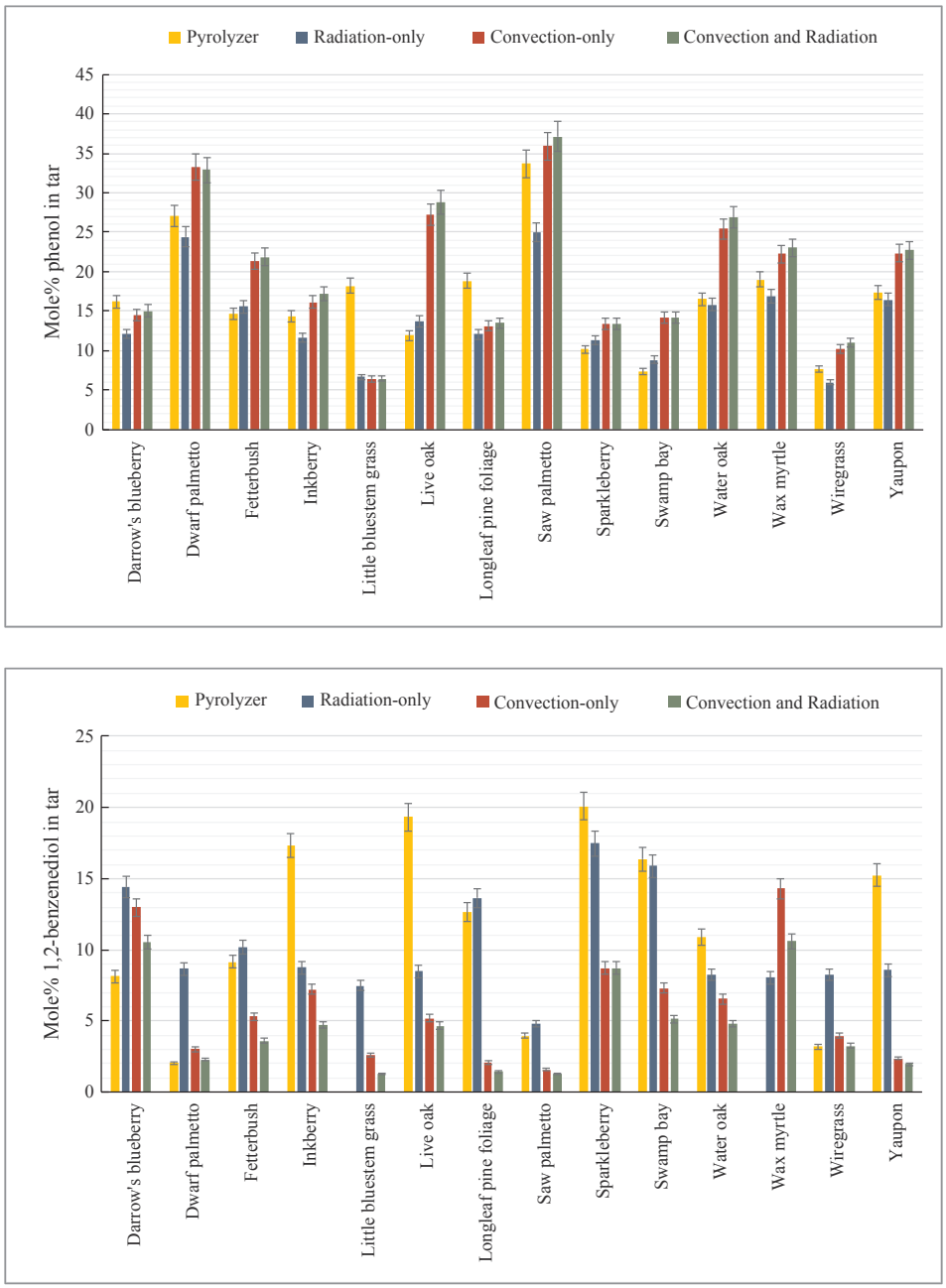

Fig. 8. Mole percent phenol (top) and 1,2-benzenediol (bottom) in tar during pyrolysis of 14 live plant species. Error bars represent the 95% confidence interval.

of phenyl groups [46]. It has also been reported that H_2 may be formed by the secondary pyrolysis of heavy hydrocarbons in the gas phase [48]. Ring condensation reactions (formation of multiple aromatic ring species from smaller aromatic species) can also expel H_2.

3.4. Tar species analysis

In the literature, several definitions for tar have been proposed. Tar is commonly defined as any pyrolysis product that condenses at room temperature and pressure. Tar has also been defined as a mixture of condensable hydrocarbon compounds, including polycyclic aromatic hydrocarbons (PAHs) and oxygen-containing hydrocarbons [49]. Tar was also defined as all hydrocarbons with molecular weights greater than benzene [50].

Milne and Evans [51] classified tar into four groups depending on pyrolysis temperature: primary, secondary, alkyl-tertiary, and condensed-tertiary. Primary tars are formed by the breakdown of the plant building blocks and consist of acids, ketones, aldehydes, alcohols, phenols, etc. Secondary tars, such as heavier phenols and olefins, are formed as the primary tars undergo secondary reactions at temperatures above 500 °C. Alkyl-tertiary tars are aromatic compounds with alkyl attachments on their rings, such as toluene, methyl naphthalene, etc. Condensed-tertiary tars include PAHs without substituents, such as pyrene, phenanthrene, etc. However, sometimes the distinctions between types of tar are not completely clear upon product analysis, such as the distinction between secondary and tertiary tar compounds [52].

During the pyrolysis of plants, three lignin units (i.e., vanillin, guaiacol, and catechol) form from the pyrolysis of lignin. The lignin units then pyrolyze or react with hydrogen to form primary tars, which include 1-ring aromatic compounds, such as benzene and phenol [53]. Primary pyrolysis reactions are completed at approximately 500 °C. At higher pyrolysis temperatures and heating rates, lower molecular weight PAHs (primary pyrolysis products) undergo secondary reactions and form heavier PAHs, such as naphthalene, anthracene, and pyrene, which are known as secondary and tertiary tars [54]. Free-radical reactions are important factors in the formation of the heavier tars (secondary and tertiary tars) from the primary tars. First, the chemical bonds in the primary tars are broken to form free radicals via homolysis reactions. Next, the radicals can react with other tar compounds to form new radicals and heavier tar compounds via ring crosslinking reactions. Then heavier PAHs can form via a series of reactions, such as hydrogen transfer reactions, isomerization reactions, etc. Finally, two radicals can react to form a stable heavy PAH via termination reactions [55,56].

During the experiments, the tars, which were condensed in the cold trap, were extracted using dichloromethane as a solvent and were analyzed using GC–MS. Fig. 7 illustrates typical tar analyses for the same plant species (longleaf pine) which were obtained in the three different heating modes. The complete results of the tar analysis for all plant species in the three heating modes are presented elsewhere [4,57]. The tar analysis indicates that the majority of the tar compounds formed in the slow-heating and radiation-only modes were primary tars, including C_5-C_{20} aliphatic molecules and 1–2 ring aromatic compounds with multiple attachments (e.g., hydroxyl (OH), methoxy (O-CH_3), etc.). The distribution of tar compounds indicates that there were no or little secondary pyrolysis reactions occurring in the radiation-only mode. However, as the pyrolysis temperature and heating rate increased during the convection-only and the combined modes, more complex tar compounds were formed, including 1- to 5-ring aromatic compounds with few attachments on their rings (known as secondary and tertiary tars).

As shown in Fig. 7, the main tar compounds in the slow-heating and radiation-only modes were phenol, 1,2-benzenediol, 1,4-benzenediol, 2-methyl phenol, 4-methyl phenol, 2,6-dimethoxy phenol. These tar compounds, which are known as primary tars, may form from the degradation of lignin, and have single aromatic rings with hydroxyl, alkyl, and methoxy attachments. Other components in the plant besides lignin, cellulose, and hemicellulose may also contribute to the tar yield. In contrast with the tar analysis in the radiation-only mode, some of the main tar compounds in the convection-only and the combined modes were naphthalene, fluorene, anthracene, phenanthrene, flouranthene, pyrene, and benzopyrene. These tar compounds are secondary and tertiary tars. However, phenol was still a major constituent of the tar in

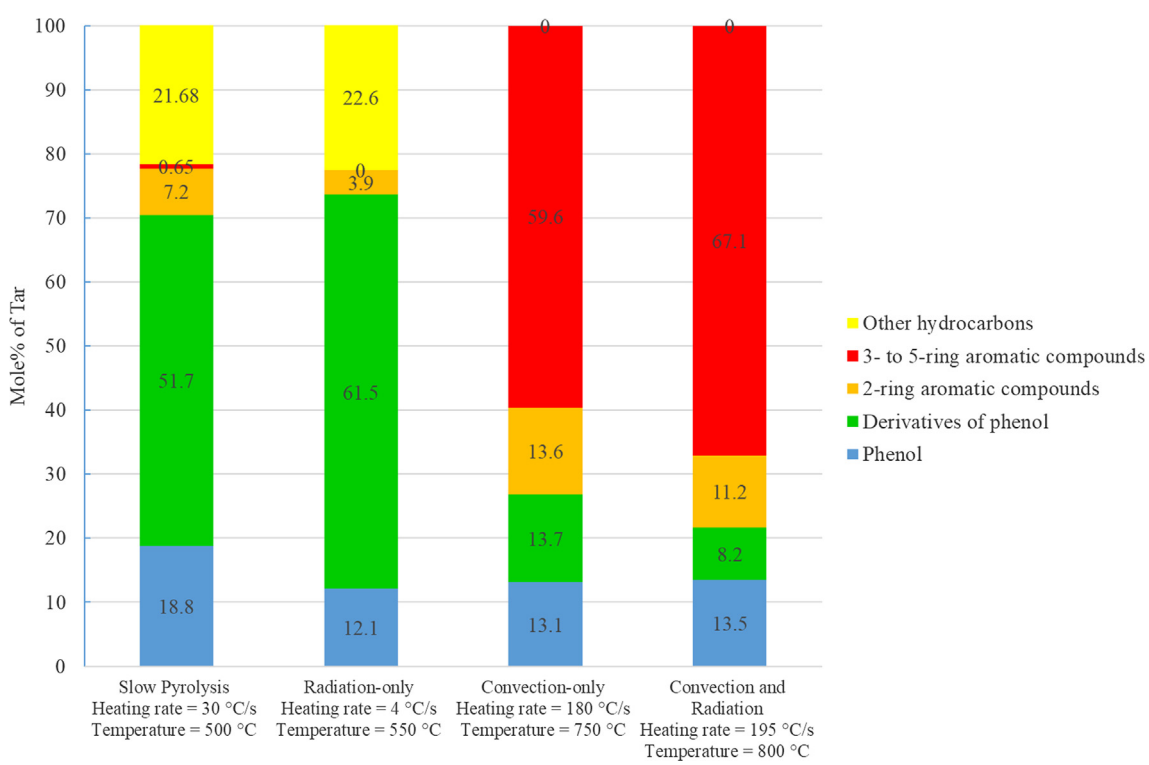

Fig. 9. Distribution of functional groups in tar for pyrolysis of live longleaf pine foliage.

the convection-only and the combined modes. In the convection-only and the combined modes, tar compounds with attachments on the aromatic rings, such as 2,6-dimethoxy phenol, 1,2,3-benzenetriol, and 4-methyl 1,2, benzenediol were observed, but in lower quantities than observed in the radiation-only mode.

In a related study, Zhang, et al. [58] noted that by increasing the pyrolysis temperature from 700 to 900 °C, the measured concentration of condensed PAHs (condensed means that the aromatic rings have one side in common) in pyrolysis tar during the pyrolysis of rice straw increased from 7 to 41%. However, this concentration then slightly decreased to 37% as temperature was increased to 1000 °C. It was also reported that the concentration of alkyl aromatics noticeably decreased at temperatures higher than 800 °C.

Fig. 7 showed results for only one plant species. Complete tar species analyses are available [4,57]. Two of the major tar species that were observed in every experiment were phenol and 1,2-benzenediol; yields of these two species are shown in Fig. 8 for all four modes of heating. The yields of each of these two tar species are quite different for each plant species, with no clear trend with heating mode that is common to all plant species.

Since there are so many individual tar species, an analysis was performed by lumping tar species into functional groups for comparison between heating modes. Fig. 9 shows the distribution of functional groups in the tar for the pyrolysis of live longleaf pine foliage in the three heating modes. The tar compounds were classified into three groups based on their molecular weight and chemical structure as follows: (1) phenol; (2) derivatives of phenol, including 1,2-benzenediol, 1,4-benzenediol, 2,6-dimethylphenol, etc.; (3) 2-ring aromatic compounds, including naphthalene, 1-methylnaphtalene, etc.; (4) 3- to 5-ring aromatic compounds, including fluoranthene, anthracene, phenanthrene, etc.; and (5) other hydrocarbons, including alcohols, ethers, esters, furans, etc.

The results shown in Fig. 9 indicate that an increase in pyrolysis temperature and heating rate had a significant effect on the distribution of the functional groups present in the collected tar. Oxygenated compounds, such as phenol (12.1 mol%) and its derivatives (61.5 mol%) made up the largest portion of tar produced in the radiation-only mode, which was performed at a lower pyrolysis temperature and heating rate. This functional group distribution in the radiation-only mode was similar to the distribution in the slow-heating mode. The remaining species in the radiation-only tar were 2-ring aromatic compounds (3.9 mol%) and other oxygenated hydrocarbons (22.6 mol%), such as alcohols, furans, ketones, etc. The primary pyrolysis tars underwent relatively few secondary reactions in the radiation-only and slow-heating modes, judging by the number of multiple ring compounds. In contrast, the convection-only and the combined modes had a significant amount of multiple aromatic ring compounds, which is evidence for secondary pyrolysis reactions.

Cracking and polymerization reactions, which are simultaneous parallel reactions, play important roles in the conversion and formation of tar compounds, especially at higher temperatures and heating rates [59]. By increasing the temperature and heating rate, the yield of phenol derivatives decreased noticeably to 13.7 and 8.2% for the convection-only and the combined modes, which indicates that the attachments to the phenol ring were removed, leading to a higher yield of phenol and also contributing to the formation of heavier PAHs. The yield of 2-ring aromatic compounds increased noticeably from 3.9 mol % (for the radiation-only) to 13.6 and 11.2 mol% for the convection-only and the combined modes, respectively. No other oxygenated hydrocarbons, such as alcohols, ketones, esters, etc. were observed in tar at high temperatures and heating rates. It has been reported that the oxygenated tars are completely decomposed and are not found at temperatures higher than 1000 °C [58].

The largest portion of the tar included 3- to 5- ring aromatic compounds for the convection-only mode (59.6 mol%) and the combined mode (67.1 mol%); indicating that the primary tars underwent secondary reaction, leading to the presence of heavier PAHs. The combined mode, which was performed at higher temperatures and heating rates compared to the convection-only mode, showed higher quantities of heavy PAHs due to the additional secondary reactions of tar compounds.

The formation of multiple-ring aromatic compounds at higher temperatures and heating rates may be due to the availability of radical sites due to the removal of attachments from the aromatic rings and then polymerization reactions [58,60]. PAHs may also form as follows: (i) the transformation of methoxyphenols to phenol by cleaving the C-O bond, (ii) then phenol may be converted to cyclopentadiene as an intermediate via the necessary decarbonylation reactions, and (iii) finally, PAHs may form from the intermediate through the Diels-Alder reactions [59,61]. PAHs may later lead to the formation of soot particles. For example, Johansson suggested a three-stage CHRCR mechanism: (1) initiator-RSR growth by radical-chain reactions, (2) hydrocarbon clustering by radical-chain reactions, and (3) particle–surface growth by radical-chain reactions [62]. A detailed model was proposed by Josephson, et al. [41] to predict soot formation from coal or biomass tar, including comparison with data.

The results in Fig. 9 are typical of the tars from all plant species studied. Tars from slow-heating and radiation-only experiments were primary tars with few 2-ring aromatic compounds and many hydroxy and methoxy attachments. Tars from the convection-only and combined modes exhibited many more 2–5 ring aromatic compounds with few attachments. However, the total tar yields and extent of conversion during pyrolysis were higher in the convection-only and combined modes. Therefore the loss of hydroxy and methoxy attachments was compensated by further degradation of the remaining char at the higher temperatures and heating rates, resulting in the net increase in tar yield.

4. Conclusion

In this study, the pyrolysis of 14 live wildland fuels was investigated in a flat-flame burner apparatus, operated under three heating modes: a radiation-only mode, a convection-only mode, and a mode combining radiation and convection. Results from a slow-heating pyrolysis experiment were also compared. The main conclusions from this study are as follows:

1- The analysis of pyrolysis product yields showed that the highest gas yields were obtained from the combined mode. The radiation-only and slow-heating modes, which were performed at lower temperatures and heating rates, led to the lowest gas yields for all plant species. The average light gas yields obtained from the pyrolysis of all plants were 20 wt% (daf) for the slow-heating and radiation-only modes, 22 wt% for the convection-only mode, and 24 wt% for the combined mode.
2- Similar to the light gas yield data, by increasing the pyrolysis temperature and heating rate, higher tar yields were obtained. The average tar yield from the pyrolysis of all plants was 53 wt% (daf) for the radiation-only mode compared to 49% for the slow-heating mode. However, tar yields were 58 and 59 wt% (daf) for the convection-only and the combined modes, respectively. The higher gas and tar yields at higher pyrolysis temperatures and heating rates were due to the further pyrolysis of char and secondary pyrolysis reactions.
3- Tar and light gas yields in the flat-flame burner system for longleaf pine litter did not follow the same trend with increasing temperature as observed in a low heating rate pyrolyzer. Significant decreases in tar yield were observed with increasing temperature in the slow-heating pyrolyzer, but tar yields increased with temperature in the higher heating rate experiments. These results imply that temperature effects alone cannot explain the changes in tar yields.
4- For all three heating modes, CO was the main light gas species on a wt% basis, followed by CO_2, CH_4, and H_2. The lowest CO yields were

observed during the radiation-only mode, and the highest in the combined mode. The average percentage of CO in the light gas from the pyrolysis of plants was 52.1 wt% (dry light gas basis) for the slow-heating mode, 53.4 wt% for the radiation-only mode, 59.8 wt % for the convection-only mode, and 63.6 wt% for the combined mode. In contrast, CO_2 yields decreased with increasing temperature and heating rate. The average CO_2 percentage of the light gas from the pyrolysis of plants was 38.4 wt% (dry light gas basis) for the slow-heating mode, 36 wt% for the radiation-only mode, 29.5 wt% for the convection-only mode, and 26.8% for the combined mode.

5- For most of the plants, differences in the H_2 yields (on a wt% of the dry light gas basis) were small and within experimental error, while some variation in CH_4 yields was observed for different plant species.

6- The distribution of tar compounds during the slow-heating and radiation-only modes were completely different than that of the convection-only and the combined modes. During the radiation-only mode, which was performed at a lower temperature and heating rate, primary tar compounds were the most prevalent compounds in the tar, which formed from the decomposition of lignin. However, during the convection-only and the combined modes, tar included phenol and a few other 1-ring compounds, but also included a significant amount of 3- to 5-ring aromatic compounds with very few attachments on the rings. The presence of these heavy polycyclic aromatic hydrocarbons (PAHs) at high temperatures and heating rates indicate that the primary tar compounds underwent secondary reactions. However, the tar yield did not decrease with temperature, which would have been expected with severe cracking of tar to light gases at elevated temperature.

7- Comparison of the yields of principal tar compounds, such as phenol and 1,2-benzenediol, showed wide variations with plant species and with heating mode, and no clear trend was observed with heating mode that was general for all plant species.

Credit authorship contribution statement

Mohammad-Saeed Safdari: Conceptualization, Methodology, Data curation, Writing - original draft, Visualization. **Elham Amini:** Methodology, Writing - review & editing. **David R. Weise:** Formal analysis, Writing - review & editing, Funding acquisition, Project administration. **Thomas H. Fletcher:** Formal analysis, Writing - review & editing, Project administration, Visualization, Supervision.

Declaration of Competing Interest

The authors declare that they have no known competing financial interests or personal relationships that could have appeared to influence the work reported in this paper.

Acknowledgements

This research was funded by DOD/EPA/DOE Strategic Environmental Research and Development Program, Project RC-2640, funded through contract 16-JV-11272167-024, administered by the USDA Forest Service PSW Research Station.

Appendix A. Supplementary data

Supplementary data to this article can be found online at https://doi.org/10.1016/j.fuel.2020.117342.

References

[1] McAllister S, Grenfell I, Hadlow A, Jolly WM, Finney M, Cohen J. Piloted ignition of live forest fuels. Fire Safety J 2012;51:133–42.
[2] Biagini E, Tognotti L. A generalized procedure for the devolatilization of biomass fuels based on the chemical components. Energy Fuel 2014;28:614–23.
[3] Amini E, Safdari MS, DeYoung JT, Weise DT, Fletcher TH. Characterization of pyrolysis products from slow pyrolysis of live and dead vegetation native to the southern United States. Fuel 2019;235:1475–91.
[4] Safdari MS. Characterization of pyrolysis products from fast pyrolysis of live and dead vegetation. Dissertation, Chemical Engineering Department. Brigham Young University; 2018.
[5] Safdari MS, Dietenberger M, Weise DR, Fletcher TH. Characterization of pyrolysis products from fast pyrolysis of live and dead vegetation native to the southern United States. Fuel 2018;229:151–66.
[6] McAllister S, Finney M. Autoignition of wood under combined convective and radiative heating. P Combust Inst 2017;36:3073–80.
[7] Wagner CEV. Calculations on forest fire spread by flame radiation. 6th World Forestry Congress. 1967. Madrid, Spain.
[8] Frankman D, Webb BW, Butler BW. Time-resolved radiation and convection heat transfer in combusting discontinuous fuel beds. Combust Sci Technol 2010;182:1391–412.
[9] Feng Y, Jiang YG, Li X, Zhang SL, Qin J, Cao Y, et al. Numerical study on the influences of heat and mass transfers on the pyrolysis of hydrocarbon fuel in mini-channel. Appl Therm Eng 2017;119:650–8.
[10] Albini FA. A model for fire spread in wildland fuels by radiation. Combust Sci Technol 1985;42:229–58.
[11] Frankman D, Webb BW, Butler BW, Latham DJ. Fine fuel heating by radiant flux. Combust Sci Technol 2010;182:215–30.
[12] Morvan D, Frangieh N. Wildland fires behaviour: Wind effect versus Byram's convective number and consequences upon the regime of propagation. Int J Wildland Fire 2018;27:636–41.
[13] Asensio MI, Ferragut L. On a wildland fire model with radiation. Int J Numer Meth Eng 2002;54:137–57.
[14] Demestre NJ, Catchpole EA, Anderson DH, Rothermel RC. Uniform propagation of a planar fire front without wind. Combust Sci Technol 1989;65:231–44.
[15] Gallacher J. The influence of season, heating mode and slope angle on wildland fire behavior. Dissertation, Chemical Engineering. Brigham Young University; 2016.
[16] Pickett BM, Isackson C, Wunder R, Fletcher TH, Butler BW, Weise DR. Experimental measurements during combustion of moist individual foliage samples. Int J Wildland Fire 2010;19:153–62.
[17] Baines PG. Physical mechanisms for the propagation of surface fires. Math Comput Model 1990;13:83–94.
[18] Weber RO. Modeling fire spread through fuel beds. Prog Energy Combust 1991;17:67–82.
[19] Carrier GF, Fendell FE, Wolff MF. Wind-aided firespread across arrays of discrete fuel-elements.1. Theory. Combust Sci Technol 1991;75:31–51.
[20] Wolff MF, Carrier GF, Fendell FE. Wind-aided firespread across arrays of discrete fuel elements.2. Experiment. Combust Sci Technol 1991;77:261–89.
[21] Zhou XY, Mahalingam S, Weise D. Modeling of marginal burning state of fire spread in live chaparral shrub fuel bed. Combust Flame 2005;143:183–98.
[22] Yedinak KM, Cohen JD, Forthofer JM, Finney MA. An examination of flame shape related to convection heat transfer in deep-fuel beds. Int J Wildland Fire 2010;19:171–8.
[23] Prince DR. Measurement and modeling of fire behavior in leaves and sparse shrubs. Dissertation, Chemical Engineering. Brigham Young University; 2014.
[24] Fang JB, Steward FR. Flame spread through randomly packed fuel particles. Combust Flame 1969;13:392–1000.
[25] Butler BW, Cohen J, Latham DJ, Schuette RD, Sopko P, Shannon KS, et al. Measurements of radiant emissive power and temperatures in crown fires. Can J Forest Res 2004;34:1577–87.
[26] Rothermel RC. A mathematical model for predicting fire spread in wildland fuels, Research Paper INT-115. Intermountain Forest and Range Experiment Station, Ogden, UT: USDA Forest Service; 1972.
[27] Safdari MS, Amini E, Weise DR, Fletcher TH. Heating rate and temperature effects on pyrolysis products from live wildland fuels. Fuel 2019;242:295–304.
[28] Gao NB, Liu BL, Li AM, Li JJ. Continuous pyrolysis of pine sawdust at different pyrolysis temperatures and solid residence times. J Anal Appl Pyrol 2015;114:155–62.
[29] Aysu T, Kucuk MM. Biomass pyrolysis in a fixed-bed reactor: Effects of pyrolysis parameters on product yields and characterization of products. Energy 2014;64:1002–25.
[30] Oudenhoven SRG, Westerhof RJM, Kersten SRA. Fast pyrolysis of organic acid leached wood, straw, hay and bagasse: Improved oil and sugar yields. J Anal Appl Pyrol 2015;116:253–62.
[31] Bridgwater AV. Review of fast pyrolysis of biomass and product upgrading. Biomass Bioenergy 2012;38:68–94.
[32] Choi HS, Choi YS, Park HC. Fast pyrolysis characteristics of lignocellulosic biomass with varying reaction conditions. Renew Energy 2012;42:131–5.
[33] Lin YH, Yan W, Sheng KC. Effect of pyrolysis conditions on the characteristics of biochar produced from a tobacco stem. Waste Manage Res 2016;34:793–801.
[34] Adrados A, Lopez-Urionabarrenechea A, Solar J, Requies J, De Marco I, Cambra JF. Upgrading of pyrolysis vapours from biomass carbonization. J Anal Appl Pyrol 2013;103:293–9.
[35] Agirre I, Griessacher T, Rosler G, Antrekowitsch J. Production of charcoal as an alternative reducing agent from agricultural residues using a semi-continuous semi-pilot scale pyrolysis screw reactor. Fuel Process Technol 2013;106:114–21.
[36] Solar J, de Marco I, Caballero BM, Lopez-Urionabarrenechea A, Rodriguez N, Agirre I, et al. Influence of temperature and residence time in the pyrolysis of woody biomass waste in a continuous screw reactor. Biomass Bioenergy 2016;95:416–23.
[37] Prins MJ, Ptasinski KJ, Janssen FJJG. Torrefaction of wood – part 1. Weight loss

kinetics. J Anal Appl Pyrol 2006;77:28–34.
[38] Lewis AD, Fletcher TH. Prediction of sawdust pyrolysis yields from a flat-flame burner using the CPD model. Energy Fuel 2013;27:942–53.
[39] Horne PA, Williams PT. Influence of temperature on the products from the flash pyrolysis of biomass. Fuel 1996;75:1051–9.
[40] Zanzi R, Sjostrom K, Bjornbom E. Rapid pyrolysis of agricultural residues at high temperature. Biomass Bioenerg 2002;23:357–66.
[41] Josephson AJ, Linn RR, Lignell DO. Modeling soot formation from solid complex fuels. Combust Flame 2018;196:265–83.
[42] Zhao B, O'Connor D, Zhang J, Peng T, Shen Z, Tsang DCW, et al. Effect of pyrolysis temperature, heating rate, and residence time on rapeseed stem derived biochar. J Clean Prod 2018;174:977–87.
[43] Haykiri-Acma H, Yaman S, Kucukbayrak S. Effect of heating rate on the pyrolysis yields of rapeseed. Renew Energ 2006;31:803–10.
[44] Sharma RK, Hajaligol MR. Effect of pyrolysis conditions on the formation of polycyclic aromatic hydrocarbons (pahs) from polyphenolic compounds. J Anal Appl Pyrol 2003;66:123–44.
[45] Torikai K, Yoshida S, Takahashi H. Effects of temperature, atmosphere and pH on the generation of smoke compounds during tobacco pyrolysis. Food Chem Toxicol 2004;42:1409–17.
[46] Yang HP, Yan R, Chen HP, Lee DH, Zheng CG. Characteristics of hemicellulose, cellulose and lignin pyrolysis. Fuel 2007;86:1781–8.
[47] Chen YQ, Yang HP, Wang XH, Zhang SH, Chen HP. Biomass-based pyrolytic polygeneration system on cotton stalk pyrolysis: Influence of temperature. Bioresource Technol 2012;107:411–8.
[48] Park WC, Atreya A, Baum HR. Experimental and theoretical investigation of heat and mass transfer processes during wood pyrolysis. Combust Flame 2010;157:481–94.
[49] Ni M, Leung DYC, Leung MKH, Sumathy K. An overview of hydrogen production from biomass. Fuel Process Technol 2006;87:461–72.
[50] Maniatis K, Beenackers AACM. Tar protocols: IEA bioenergy gasification task. Biomass Bioenerg 2000;18:1–4.
[51] Milne TA, Evans RJ, Biomass gasifier “tars”: their nature, formation, and conversion, NREL; 1998.
[52] Rios MLV, Gonzalez AM, Lora EES, del Olmo OAA. Reduction of tar generated during biomass gasification: A review. Biomass Bioenerg 2018;108:345–70.
[53] Farag S, Fu DB, Jessop PG, Chaouki J. Detailed compositional analysis and structural investigation of a bio-oil from microwave pyrolysis of Kraft lignin. J Anal Appl Pyrol 2014;109:249–57.
[54] Shen YF, Wang JF, Ge XL, Chen MD. By-products recycling for syngas cleanup in biomass pyrolysis - an overview. Renew Sust Energ Rev 2016;59:1246–68.
[55] Zhou H, Wu CF, Onwudili JA, Meng AH, Zhang YU, Williams PT. Polycyclic aromatic hydrocarbons (pah) formation from the pyrolysis of different municipal solid waste fractions. Waste Manage 2015;36:136–46.
[56] Feng DD, Zhao YJ, Zhang Y, Sun SZ. Effects of H_2O and CO_2 on the homogeneous conversion and heterogeneous reforming of biomass tar over biochar. Int J Hydrogen Energ 2017;42:13070–84.
[57] Amini E. Characterization of pyrolysis products from slow pyrolysis of live and dead vegetation, PhD Dissertation. Chemical Engineering Dept.: Brigham Young University; 2019. (in progress).
[58] Zhang Yl, Wu WG, Zhao SH, Long YF, Luo YH. Experimental study on pyrolysis tar removal over rice straw char and inner pore structure evolution of char. Fuel Process Technol 2015;134:333–44.
[59] Jess A. Mechanisms and kinetics of thermal reactions of aromatic hydrocarbons from pyrolysis of solid fuels. Fuel 1996;75:1441–8.
[60] Palma CF. Modelling of tar formation and evolution for biomass gasification: A review. Appl Energ 2013;111:129–41.
[61] Nowakowska M, Herbinet O, Dufour A, Glaude P-A. Detailed kinetic study of anisole pyrolysis and oxidation to understand tar formation during biomass combustion and gasification. Combust Flame 2014;161:1474–88.
[62] Johansson KO, Head-Gordon MP, Schrader PE. Resonance-stabilized hydrocarbon radical chain reactions may explain soot inception and growth. Science 2018;361:997–1000.